LAWRENCE
LIVERMORE
NATIONAL
LABORATORY

LLNL-JRNL-753800

Detailed Modeling of Fission with FREYA

R. Vogt, J. Randrup

June 27, 2018

Nuclear Instruments and Methods A

Disclaimer

Detailed Modeling of Fission with FREYA

R. Vogt

Nuclear and Chemical Sciences Division, Lawrence Livermore National Laboratory, Livermore, CA 94551, USA

Physics Department, University of California at Davis, Davis, CA 95616, USA

J. Randrup

Nuclear Science Division, Lawrence Berkeley National Laboratory, Berkeley, CA 94551, USA

Abstract

For many years, the state of the art for treating fission in radiation transport codes has involved sampling from average distributions. However, such average fission models have limited interaction-by-interaction capabilities. Energy is not explicitly conserved and no correlations are available because all particles are emitted isotropically and independently. However, in a true fission event, the energies, momenta and multiplicities of emitted particles are correlated. Such correlations are interesting for many modern applications, including detector development and detection of small amounts of special material. Recently, several Monte Carlo codes have become available that calculate complete fission events. Event-by-event techniques are particularly useful because it is possible to obtain the fission products as well as the prompt neutrons and photons emitted during an individual fission process, all with complete kinematic information. It is therefore possible to extract any desired correlation observables. Such codes, when included in broader Monte Carlo transport codes, such as MCNP, can be made broadly available to the community. One such code, FREYA (Fission Reaction Event Yield Algorithm), is particularly fast and can readily generate large samples of complete fission events. We briefly describe the physics in FREYA and compare our results with relevant available data on prompt neutron and photon emission. We discuss correlated measurements in particular for validation.

Preprint submitted to Nuclear Instruments & Methods in Physics Research August 2, 2018

Keywords: nuclear fission, correlations, fission simulations

1. Introduction

FREYA was developed to provide a fast event-by-event framework to model complete fission events. Event-by-event modeling has been used in other fields of physics where there are a large variety of outcomes to study detector response and predict experimental results. This framework is readily adaptable to fission studies. The FREYA event output includes full kinematic information on the two product nuclei as well as all the emitted neutrons and photons. It was the first such published fission model made publicly available [1]. FREYA version 2.0.2 is now available in Ref. [2]. For a recent review and discussion of other available fission codes, see Ref. [3]. The advantage of having samples of complete events is that it is straightforward to extract any observable, including fluctuations and correlations, and to take account of detector acceptances and cuts. Previously, transport codes sampled the neutron energies from the same spectral distribution and thus provided no correlated information.

2. How FREYA Works

As input, FREYA requires the mass distribution of the primary fission fragments, $Y(A)$, and the mean total kinetic energy for a given mass split, $\overline{\mathrm{TKE}}(A)$, for the particular excitation considered. (FREYA can simulate both neutron-induced fission and spontaneous fission.)

For a given split of nucleus A_0 into light and heavy fragments, L and H respectively, the Q-value is given by $Q = M_0c^2 - M_Lc^2 - M_Hc^2$. For a given total fragment kinetic energy TKE, the total excitation energy available for rotational and statistical excitation of the dinuclear complex at scission is then $E^*_{\mathrm{sc}} = Q - \overline{\mathrm{TKE}}$ and the corresponding 'scission temperature' T_{sc} is obtained from $E^*_{\mathrm{sc}} = a(A_0)T^2_{\mathrm{sc}}$, where the scale of the level density parameter $a(A) = A/e_0$ is governed by $e_0 \approx 10\,\mathrm{MeV}$, the first adjustable parameter in FREYA.

In addition to any overall rigid rotation, which imparts mean angular momenta to the two fragments, the fragments also acquire fluctuations around those mean values from the dinuclear wriggling and bending modes. The magnitude of these spin fluctuations is governed by the 'spin temperature' $T_S = c_S T_{\rm sc}$ which can be adjusted by means of the second `FREYA` parameter c_S. The spin fluctuations vanish for $c_S = 0$, while $c_S = 1$ leads to the average fragment angular momenta $\overline{S}_L \approx 6.2\hbar$ and $\overline{S}_H \approx 7.6\hbar$ for ^{252}Cf(sf).

After subtracting for the rotational energy of the two fragments, $E_{\rm rot}$, one is left with a total of $E_{\rm stat} = E^*_{\rm sc} - E_{\rm rot}$ for statistical fragment excitation which is distributed between the two fragments. A preliminary partition, $E_{\rm stat} = \acute{E}^*_L + \acute{E}^*_H$, is made according to the heat capacities of the fragments, assumed to be proportional to the level density parameters, *i.e.* $\acute{E}^*_L : \acute{E}^*_H = a_L : a_H$. If the shell corrections are negligible, or the available energy is large, $a_i \approx A_i/e_0$.

Because the observed neutron multiplicities suggest that the light fragments tend to be disproportionately excited, the average excitations are modified in favor of the light fragment, $\overline{E}^*_L = x\acute{E}^*_L$, $\overline{E}^*_H = E_{\rm stat} - \overline{E}^*_L$, where the third `FREYA` parameter x is expected be somewhat larger than unity.

After the mean fragment excitation energies have been assigned, `FREYA` considers thermal fluctuations. The mean fragment excitation is related to its temperature T_i by $\overline{E}^*_i = a_i T_i^2$ and its associated variance is $\sigma^2_{E_i} = 2\overline{E}^*_i T_i$. An energy fluctuation δE^*_i is sampled from a truncated normal distribution of variance $2c\overline{E}^*_i T_i$ and the fragment excitations are adjusted accordingly, $E^*_i = \overline{E}^*_i + \delta E^*_i$, $i = L, H$. Energy conservation is accounted for by making a compensating opposing fluctuation in the total kinetic energy, $\mathrm{TKE} = \overline{\mathrm{TKE}} - \delta E^*_L - \delta E^*_H$. The factor $c > 1$ multiplying the variance is the fourth `FREYA` parameter; it compensates for the truncation of the normal distribution due to energy conservation. Finally, TKE may be adjusted by the fifth `FREYA` parameter, dTKE, to ensure reproduction of the average neutron multiplicity, $\overline{\nu}$.

The neutrons are evaporated isotropically in the frame of the emitting fragment, apart from a slight flattening due to the nuclear rotation. Their energy is sampled from a black-body energy spectrum, $dN_n/dE_n \sim E_n \exp(-E_n/T_{\rm max})$,

where $T_{\max}$ is the maximum possible temperature in the daughter nucleus. `FREYA` generally assumes that neutron evaporation continues until the nuclear excitation energy is below the neutron separation energy $S_{\rm n}$, so that neutron evaporation continues as long as energetically possible.

After neutron evaporation has ceased, the excited product nucleus emits photons. First statistical photons are emitted isotropically with an energy distribution sampled from a black-body spectrum modulated by a giant-dipole resonance form factor. When the yrast line is reached, a sequence of collective emissions follow. When the nuclear excitation energy enters the regime of the tabulated decays from the RIPL-3 compilation [4], `FREYA` switches to a discrete cascade which is continued until the half-life exceeds a specified value, $t_{\max}$, based on the detector response time.

The five `FREYA` parameters, e_0, c_S, x, c and dTKE, are all physics-based and affect some observables directly without having any significant effect on others. For example, c_S, the parameter related to spin fluctuations, controls the photon energy and multiplicity but has a negligible effect on the neutron observables. (The only effect of c_S on neutron emission comes from the fact that it controls the division of the total excitation energy into rotational and statistical excitation. Giving more energy to rotation by a large c_S reduces the statistical energy for neutron emission.) The parameter x controlling the excitation energy advantage given to the light fragment has a direct effect on the neutron multiplicity as a function of fragment mass, $\nu(A)$, while, *e.g.* having no effect on the neutron multiplicity distribution $P(\nu)$. The parameter x is also the only parameter to have a strong effect on the neutron-neutron angular correlations, as will be discussed later. The parameter controlling the width of the thermal fluctuations, c, conversely, has a strong effect on $P(\nu)$ and its moments but no effect on $\nu(A)$. All the parameters, however, have some effect on the prompt fission neutron spectrum because all affect the energy available for neutron emission, either directly, as through c_S and dTKE, or indirectly, through the excitation energy sharing via x or the fluctuations controlled by c. Indeed, the only observable that is affected by e_0 is the neutron spectrum. See

Refs. [5, 6] for more discussion of how the parameter choices affect observables.

A first attempt to make a global fit of the five FREYA parameters was made in Ref. [7] using a grid search method. More recently an optimization using simulated annealing was able to generally reproduce these results as well as provide variances and covariance on the parameter values [8]. Similar studies were carried out for all spontaneous fission isotopes in FREYA.

It is interesting to note that the more empirical parameter values in the recently released version of FREYA [2] are in rather good agreement with those found using the numerical optimization in Ref. [8]. This is particularly interesting because there is really only sufficient data for a full optimization of the parameters for ^{252}Cf(sf). In some cases, the only available data for optimization are evaluations of $P(\nu)$ and the associated neutron multiplicity moments [9]. It was found that e_0, x, and c_S showed only small isotope to isotope variations while c and dTKE could have considerable variations. The strong isotope dependence of c occurs mainly for isotopes with low average neutron multiplicities, $\overline{\nu} \sim 2$, while the variation of dTKE may be in part due to the low statistics data available, sometimes without uncertainties. See Ref. [8] for more details.

The work in Ref. [8] is being extended to neutron-induced fission reactions which pose additional challenges, such as the energy dependence of the parameters. For example, one may expect e_0 to be energy independent, along perhaps, with c_S since the neutron separation energy provides a cutoff for neutron emission, independent of incident neutron energy. However, c and x may depend on neutron energy since $P(\nu)$ may broaden with increased $\overline{\nu}$ at higher energy for neutron-induced fission while it is known that the 'sawtooth' shape of $\nu(A)$ softens with increasing neutron energy. However, there are almost no data to use for optimization above thermal neutron-induced fission.

3. Illustrative Results

Correlations between emitted neutrons, photons, and fragments present some of the most informative observables that can be studied by FREYA and codes like

it. Several examples of FREYA results are given here.

3.1. Photon emission

First, results on the improved photon emission included in FREYA from Ref. [6] are presented. Figure 1 shows the prompt fission photon spectrum for ^{252}Cf(sf) measured by Billnert *et al.* [10]. They used two different detectors: lanthanum bromide, for timing and energy resolution, and cesium bromide, because of the absence of intrinsic photon activity in this material. They were able to reduce the uncertainties of their measurement considerably relative to previous results [10]: $N_\gamma = 8.30 \pm 0.08$; $E_\gamma = 6.64 \pm 0.08$ MeV; and $E_\gamma/N_\gamma = 0.80 \pm 0.01$ MeV. The results for the two different detector materials agree. The same energy cutoff, $g_{\min} = 0.1$ MeV, and time window, $t_{\max} = 1.5$ ns, is used in the FREYA calculations as in the measurement.

The calculated photon spectrum is normalized to the total calculated multiplicity, $N_\gamma = 8.37$, obtained for the $g_{\min}$ and $t_{\max}$ used by Billnert *et al.*. The overall agreement, shown on the left-hand side of Fig. 1 is very good. (Note that the uncertainties on the measurement, shown for the lanthanum bromide detectors, are not included in the plot. With these included, the apparent agreement would improve. Incorporating the GDR into FREYA provides the harder spectrum for high energy continuum emission, as exhibited in the data. Note also that the low energy end of the photon spectrum, emphasized on the right-hand side of Fig. 1, shows rather good agreement with the position of the peaks in the low energy spectral data due to the inclusion of the discrete transitions in the RIPL-3 library [6]. The average photon energy calculated with FREYA,, $\langle E_\gamma \rangle = 7.09$ MeV, is higher that that measured by Billnert *et al.*. Thus even though the calculated photon multiplicity is within the uncertainties of the data, the higher photon energy from FREYA results in a higher average energy per photon $E_\gamma/N_\gamma = 0.85$ MeV.

3.2. Correlations

In this subsection, results on neutron correlations with neutrons, light fragments, and photons are discussed. First, the origin of the shapes of the neutron-

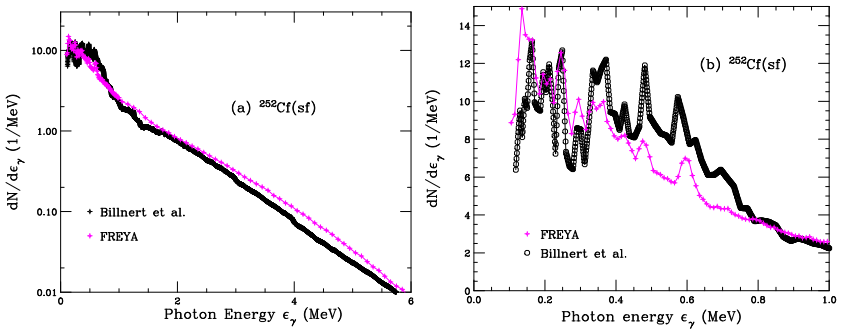

Figure 1: (Color online) The photon energy spectrum calculated for ^{252}Cf(sf) compared to data from Billnert *et al.* [10]. The total photon spectrum is shown on the left-hand side while the spectrum for energies less than 1 MeV are shown on the right-hand side. Both spectra are normalized to the fission photon multiplicity. The calculations are from Ref. [6].

neutron and neutron-light fragment angular correlations are shown in Fig. 2. The calculations shown in this figure should be taken as illustrative only. The results are then compared to some of the available data in Fig. 3. Neutron-photon correlations are discussed in Fig. 4.

3.2.1. neutron-neutron and neutron-light fragment correlations

The strong correlation between two neutrons and between neutrons and light fragments arises from the boost. Neutron emission in the fragment rest frame is isotropic. However, when boosted to the lab frame, the neutrons follow the parent fragment. On the left-hand side of Fig. 2, the various sources of two-neutron correlations are shown as a function of the relative angle between the two neutrons, ϕ_{12}. If one neutron from each fragment is used to form the correlation, then the correlation peaks at $\phi_{12} = 180$ degrees because energy conservation dictates that, in binary fission, the fragments are 180 degrees away from each other. However, if both neutrons are emitted from the same fragment, the correlation peaks at $\phi_{12} = 0$. The correlated yield is higher if both neutrons are from the light fragment because momentum conservation gives the light fragment higher velocity than the heavy fragment. When taken together, the result is the dashed black line with peaks at $\phi_{12} = 0$ and 180 degrees and

a minimum near 90 degrees. The correlation is complex and depends on the minimum energy of the detected neutrons and the neutron multiplicity. Higher neutron multiplicities can weaken the observed correlation. See Refs. [5, 11] for results and comparisons of FREYA to data.

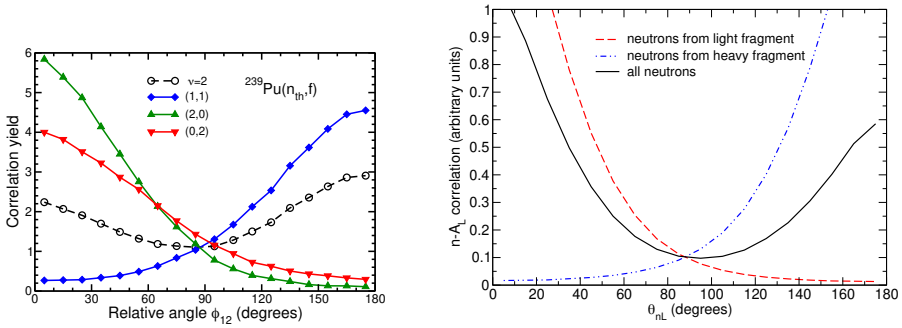

Figure 2: (Color online) *Left:* FREYA calculations shown for the angular correlation between two neutrons with kinetic energy greater than 1 MeV emitted from ^{239}Pu($n_{\rm th}$,f). The correlation for one neutron emitted from each fragment is shown in blue while that for both neutrons emitted from the light fragment and the heavy fragment are shown in the green and red curves respectively. The correlation for all neutron pairs is given by the dashed black curve. *Right:* FREYA calculations shown for neutrons emitted from ^{252}Cf(sf) correlated with the light fragment, A_L. The neutrons emitted from the light fragment (dashed red) and those emitted from the heavy fragment (dot-dot-dashed blue) are compared to the correlation of all neutrons with the light fragment. All neutrons have a minimum kinetic energy of 0.5 MeV.

While not included in the calculations, in reality, neutrons can rescatter between detectors, especially nearest neighbor detectors in an array, making a single neutron look like two neutrons. This can cause a false correlation at zero degrees, referred to as cross talk. To see the true correlation at low angles, this cross talk has to be eliminated. One method for doing so is discussed in Ref. [11].

The boost from the fragment rest frame to the lab frame also dictates the shape of the neutron-light fragment correlation shown on the right-hand side of Fig. 2, in this case shown for the angle between the neutron and the light fragment, θ_{nL}. If the neutron is emitted from the light fragment, the correlation

peaks at $\theta_{nL} = 0$ while if the neutron is emitted from the heavy fragment, the correlation peaks at $\theta_{nL} = 180$ degrees. Again the higher velocity of the light fragment causes a larger correlation at 0 degrees relative to 180 degrees, as shown in the black curve.

Comparison with selected data for neutron-neutron and neutron-light fragment correlations are shown in Fig. 3. For more results, see Ref. [3].

The left panel of Fig. 3 shows the angular correlation between two neutrons emitted during spontaneous fission of ^{240}Pu. The data were taken with an array of 77 detectors over 23 hours [11] and the number of `FREYA` events simulated was chosen to give similar statistics for the simulation and the measurement. `FREYA` is in good agreement with the data which has been used to fix the parameter x for this isotope [11]. Note that for the best comparison between the data and the calculations, `FREYA` has to be included in a simulation with the full detector setup, as was done in Ref. [11]. The need to use `FREYA` in studies of detector response was taken into account when developing `FREYA`: special attention was paid to making the code fast to be able to use it in larger transport codes.

In 1962 Bowman et al. made the first measurement of correlations between neutrons and light fragments [12]. They employed two neutron detectors and two fission fragment detectors mounted around a steel drum with a diameter of 2 m. A ^{252}Cf(sf) source was placed in vacuum at the center of the drum. The fragment detectors were mounted on opposite sides of the drum. One neutron detector was held fixed at $\theta = 11.25$ degrees while the other was moved through $22.5 < \theta < 90$ degrees with respect to one fragment detector ($111.5 < \theta < 180$ degrees relative to the other fragment detector). Time of flight was used to detect one neutron in coincidence with two fission fragments and to separate the fragments from each other. They presented the angular correlation between all measured neutrons and the identified light fragment. While the correlation is made with the light fragment, it was not possible to determine which fragment emitted the neutron [12].

The Bowman data are in good agreement with the calculations, as shown in the right-hand side of Fig. 3. The somewhat later data by Skarsvag and

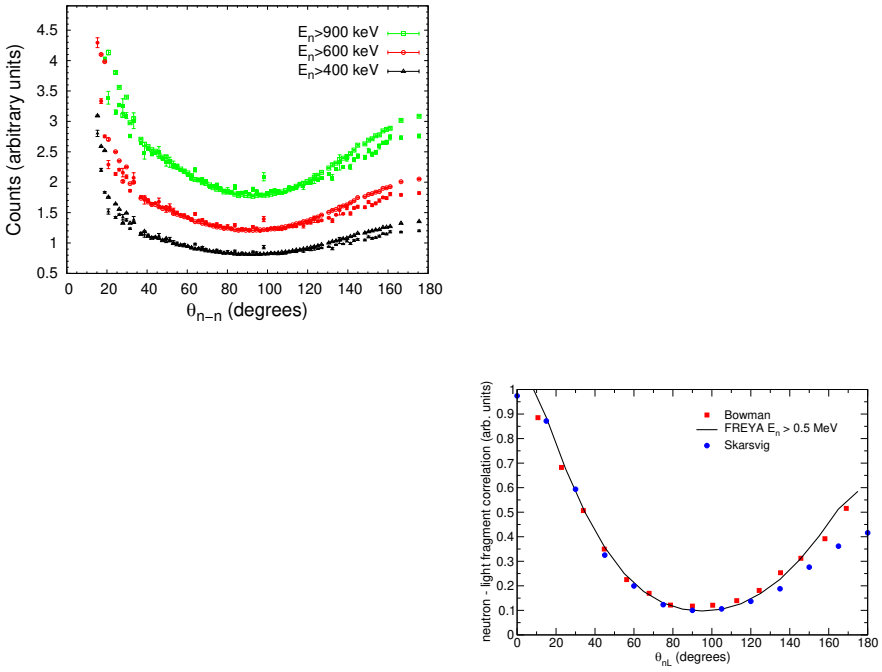

Figure 3: (Color online) *Left:* The neutron-neutron angular correlation for outgoing neutron energies greater than 400 (black), 600 (red) and 800 (green) keV. The open symbols are the `FREYA` results while the filled symbols are the data, see Ref. [11]. *Right:* The default FREYA calculations compared to ^{252}Cf(sf) neutronlight fragment angular correlation data from Refs. [12] (red squares) and [13] (blue circles). The minimum kinetic energy of the neutrons is 0.5 MeV. From Ref. [5].

Bergheim [13] differ from the Bowman data and the calculations at $\theta_{nL} > 90$ degrees. For comparison to more recent data with specific A_L, see Ref. [3].

3.2.2. neutron-photon correlations

While there is clearly a strong correlation between neutrons and neutrons with a particular fragment, one might expect a weak to nonexistent angular correlation between neutrons and photons. This is because photons always travel with the speed of light so that their emission is frame independent, it is always isotropic. However, one may look for correlations in other ways. There have been five measurements of neutron-photon correlations [14–18] in ^{252}Cf(sf), with conflicting results.

Nifenecker *et al.* [14] averaged photon and neutron measurements over fragment properties. They concluded that there was a positive linear relationship between the average total photon energy and the average number of neutrons emitted for a given fragment. They suggested that their positive correlation is evidence of an increase in the mean spin of the fragments with excitation energy.

Wang *et al.* [15] correlated photon and neutron multiplicities with total kinetic energy over three fragment mass regions of interest: light ($85 < A < 123$), symmetric ($124 < A < 131$), and heavy ($132 < A < 167$). The light and symmetric mass regions exhibit a linear trend with a positive slope, qualitatively consistent with Nifenecker, whereas the heavy mass region is nonlinear with an overall positive trend. A comparison was made with `FREYA` which showed that `FREYA` followed the general trend when using the same binning mass and total kinetic energy but the overall agreement was rather poor.

Glässel *et al.* [16] studied correlations between neutron and photon multiplicities on a fission-by-fission basis as well as based on averages, as did Nifenecker *et al.*. On average, they found that the photon multiplicity distribution was rather independent of mass. They also found that, event-by-event, there was decrease in neutron multiplicity per emitted photon, suggesting that neutron multiplicity and photon energy are anti-correlated.

Bleuel *et al.* [17] found no significant correlation between neutron and pho-

ton multiplicity. They isolated the photon multiplicity distributions for two post-neutron emission fragment pairings: two-neutron ^{106}Mo+^{144}Ba and four-neutron ^{106}Mo+^{142}Ba. With limited statistics, they found no difference in the photon multiplicities for the two- and four-neutron distributions.

While, as already mentioned, `FREYA` can obtain a weak positive correlation when the neutron and photon emission is averaged over certain mass and total kinetic energy bins, on average, it would predict a negative correlation between neutron and photon multiplicities so that the average photon multiplicity would decrease as the neutron multiplicity was increased [6].

Most recently, Marcath *et al.* [18] focused on observing neutron-photon correlations on an event-by-event basis rather than averaged over fragment mass or energy to investigate neutron-photon competition. The idea was to determine whether the number of photons detected in a given fission event has any bearing on the number of neutrons detected. The measured event-by-event correlations between neutron and photon emission were found to be weak.

The results are shown in Fig. 4. The data are compared to `CGMF` [19] and `MCNPX` − `PoliMi` [20] as well as `FREYA`. The results for the expected number of photon detected given a certain number of neutrons detected in coincidence is shown on the left-hand side while the expected number of neutrons detected for a given number of photons detected in coincidence is shown on the right-hand side. The calculations agree reasonably well with the data from Ref. [18], and with the previous measurement by Glässel. However, the translation of the Niefenecker data to this correlation display a significant discrepancy to both the data and the models (see Ref. [18]).

4. Conclusions

New advances in fission phenomenology, such as `FREYA`, open up a host of new observables. Complete event models like `FREYA` can be used both in detector response as well as in data analysis. The codes, which are in generally good agreement with data, are evolving and subject to more stringent tests as

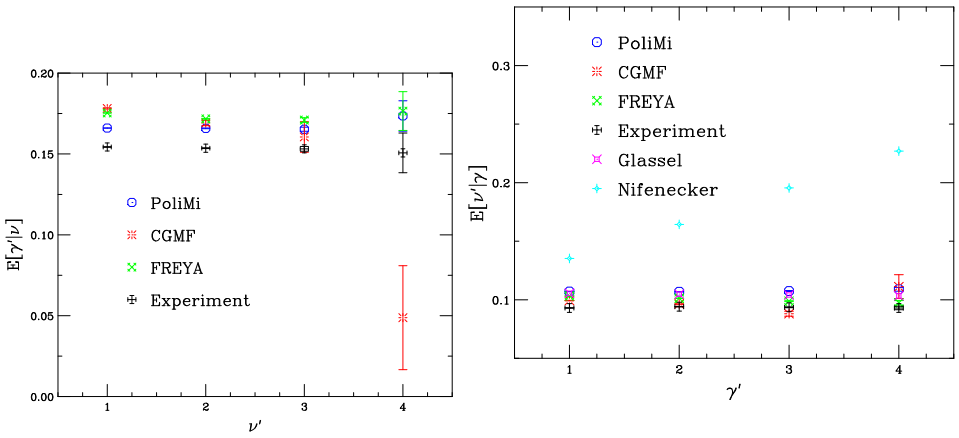

Figure 4: (Color online) *Left:* The expected number of detected photons as a function of the number of neutrons detected in coincidence. *Right:* The expected number of detected neutrons as a function of the number of photons detected in coincidence. Both results are from Ref. [18].

more correlated data become available. See Ref. [3] for more discussion and comparison with data.

Acknowledgments

R. V. would like to thank the conference organizers for the invitation to speak about this work. The work of R. V. was performed under the auspices of the U.S. Department of Energy by Lawrence Livermore National Laboratory under Contract DE-AC52-07NA27344. The work of J. R. was performed under the auspices of the U.S. Department of Energy by Lawrence Berkeley National Laboratory under Contract DE-AC02-05CH11231. This work was supported by the Office of Defense Nuclear Nonproliferation Research & Development (DNN R&D), National Nuclear Security Administration, U.S. Department of Energy.

References

[1] J. Verbeke, R. Vogt, and J. Randrup, Comp. Phys. Comm. **191** (2015) 178.

[2] J. Verbeke, R. Vogt, and J. Randrup, Comp. Phys. Comm. **222** (2018) 263.

[3] P. Talou *et al.*, Eur. Phys. J. A **54** (2018) 9.

[4] R. Capote *et al.*, Nucl. Data Sheets **110**, 3107 (2009).

[5] R. Vogt and J. Randrup, Phys. Rev. C **90** (2014) 064623.

[6] R. Vogt and J. Randrup, Phys. Rev. C **96** (2017) 064620.

[7] R. Vogt *et al.*, Proc. 1st ANS Advances in Nuc. Nonpro. Tech. and Policy, Santa Fe, NM, 2016, LLNL-CONF-690741.

[8] J. Van Dyke, L. A. Bernstein, and R. Vogt, in preparation.

[9] P. Santi and M. Miller, Nucl. Sci. Eng. **160** (2008) 190.

[10] R. Billnert, F.-J. Hambsch, A. Oberstedt, and S. Oberstedt, Phys. Rev. C **87** (2013) 024601.

[11] J. M. Verbeke, L. F. Nakae, and R. Vogt, Phys. Rev. C **97** (2018) 044601.

[12] H. R. Bowman *et al.*, Phys. Rev. **126** (1962) 2120; Phys. Rev. **129** (1963) 2133.

[13] K. Skarsvag and K. Bergheim, Nucl. Phys. **45** (1963) 72.

[14] H. Nifenecker *et al.*, Nucl. Phys. A **189** (1972) 285.

[15] T. Wang *et al.*, Phys. Rev. C **93** (2016) 014606.

[16] P. Glssel, *et al.*,, Nucl. Phys. A **502** (1989) 315.

[17] D. L. Bleuel *et al.*, Nucl. Instrum. Methods Phys. Res., Sect A **624** (2010) 691.

[18] M. J. Marcath *et al.*, Phys. Rev. C **97** (2018) 044622.

[19] P. Talou, T. Kawano, and I. Stetcu, Tech. Rep. LA-CC-13-063, Los Alamos National Laboratory (2013).

[20] S. A. Pozzi, *et al.*, Nucl. Instrum. Methods Phys. Res., Sect A **513** (2003) 550; **694** (2012) 119.